Hindawi
Journal of Chemistry
Volume 2023, Article ID 6624295, 11 pages
https://doi.org/10.1155/2023/6624295

*Research Article*

# Synthesis of Nanoporous Biochar from Rice Husk for Adsorption of Methylene Blue

**Dan Dang,[1] Lei Mei,[2] Gaimeng Yan,[1] and Wenju Liu[1]**

[1]*School of Chemistry and Chemical Engineering, Henan University of Technology, Zhengzhou 450001, China*
[2]*State Power Investment Corporation Science and Technology Research Institute Co., Ltd., South of Park Future Science City, Changping District Beijing, Beijing 100029, China*

Correspondence should be addressed to Wenju Liu; wenjuliu@haut.edu.cn

Received 8 February 2023; Revised 7 March 2023; Accepted 24 April 2023; Published 22 September 2023

Academic Editor: Liviu Mitu



In this study, rice husk charcoal prepared with KOH and KOH-NaOH as activators were investigated as adsorbents for the removal of methylene blue from aqueous solutions in order to improve the utilisation of rice husk. Firstly, the rice husk carbon was morphologically and chemically characterised using scanning electron microscopy, specific surface area analyser, and infrared spectroscopy. Secondly, the effects of the alkali-carbon ratio, pyrolysis temperature, and pyrolysis time on the activation of KOH alone and combined activation of KOH-NaOH were investigated. The results showed that the adsorption capacity of the activated biochar was 359.7 mg/g (higher than that of 315.4 mg/g when KOH alone was activated) under the same adsorption conditions when KOH-NaOH was coactivated. Finally, combined with the characterization results and data analysis, it can be seen that the rice husk carbon obtained by KOH-NaOH composite activation is predominantly microporous with a more uniform pore size distribution, making it an economical and efficient adsorbent for the removal of methylene blue from aqueous solutions.

## 1. Introduction

Water is vital to human survival. With increased urbanisation and industrialisation, water resources are heavily polluted [1]. Due to limited fresh water resources, one billion people currently do not have access to safe drinking water. In recent years, with the rapid development of the dye industry, the number and types of dyes are increasing, the composition is becoming more complex, and a large amount of water is consumed in the dyeing process, thus inevitably producing a large amount of industrial wastewater containing dyes in the process of dye production and use, and causing serious damage to the ecosystem [2, 3]. The large amount of dye effluent not only causes serious damage to the existing ecological environment and water resources but also poses a threat to aquatic life and human health [4]. The high chromaticity of dye wastewater, which can reach 500–500000, produces visual pollution to a certain extent. The inflow into the water body will reduce the light permeability of the water body, leading to the weakening of the incident light intensity, affecting the photosynthesis of aquatic organisms, reducing the dissolved oxygen content of the water body, increasing the biological oxygen demand (BOD) and chemical oxygen demand (COD), which in turn affects other aquatic organisms and breaks the ecological balance of the water body [5]. Various salts are used in the production and processing of dyestuffs, increasing the total dissolved solids (TDS) in wastewater. The presence of TDS in wastewater can alter the osmotic balance and lead to swelling or dehydration of aquatic organisms, which can lead to death [6]. Some of the dyestuffs themselves, their degradation products, and the toxic substances contained in the dye effluent have a "triple-causing" effect and pose a serious risk to human health. Under certain conditions, azo dyes can reduce certain aromatic amines, which are carcinogenic to humans or animals [7].

With the general improvement of people's awareness of environmental protection, the potential toxicity and visibility of dye wastewater have caused more attention [8, 9]. Various methods of removing and treating dyes wastewater

have been used to reduce the impact on the environment [10, 11]. Adsorption is the most effective, simple, and low-pollution way among many methods [12, 13]. Among the adsorbent materials, activated carbon is considered to be one of the most widely developed adsorbents owing to its high porosity, large specific surface area, good surface activity, and chemical stability [14, 15]. However, commercial activated carbon, which is mainly made from coal and wood, etc., is costly and its use is limited [16]. So researchers look for low-cost adsorbent materials as an alternative to activated carbon [17]. In the past, agricultural waste was often buried or burnt in the open, which had a negative impact on human health and the environment. However, there has been a trend to reuse this agricultural waste as a feedstock for various energy and environmental applications [18]. The synthesis and application of high performance biomass and biochar has received widespread attention in order to make high value use of biomass resources and reduce environmental pollution. Biochar is a solid produced by ultrahigh temperature decomposition of organic materials (pyrolysis) in partial or complete absence of oxygen, which contains elemental carbon and is physically stable. Due to its high specific surface area, high porosity, and high surface charge concentration, as well as its low price and abundant sources of raw materials, it has been widely used for the adsorption of organic and inorganic pollutants in wastewater. Biomass resources (e.g. nut shell [19, 20], waste bamboo [21], palm oil waste [22], maize straw [23], coir pith [24], Jatropha curcas husk [25], rice husk [26], etc.), which are low cost, readily available, renewable, and widely sourced, are potential materials for the preparation of activated carbon for the removal of dye wastewater.

Recently, many researchers have examined the modification of biochar to improve its adsorption performance [27]. Jawad et al. [28] used KOH as a chemical activator to convert dragon fruit peel into activated biochar, and the maximum adsorption capacity of methylene blue (MB) was 195.2 mg/g at 50°C. Malik et al. [29] prepared rice husk, rice husk biochar, and chemically modified rice husk biochar for adsorption of Congo red dye. The activated biochar was 98.9% effective in removal of Congo red dye at pH 6. Do et al. [30] used NaOH modified Moringa oleifera leaf to prepare activated biochar to remove MB from aqueous solution. The study showed that the maximum adsorption capacity for MB was 136.99 mg/g when the pH was 7 and the adsorbent dosage was 1.67 g/L. Activated biochar was mainly prepared by chemical activation and physical activation methods, of which, $ZnCl_2$, KOH, and NaOH are commonly used as activators to produce activated biochar with high specific surface area [31–33]. NaOH and KOH are commonly used for lignocellulosic biomass chemical activation [34]. However, the activation effect of combined activation of KOH-NaOH on activated biochar is rarely reported. Rice husk, a low-cost lignocellulosic agricultural waste, accounts for 15% to 20% of rice production. It contains approximately 32% cellulose, 21% hemicellulose, 21% lignin, etc. [35]. This shows that rice husk has a high cellulose content and is a polymer containing three active hydroxyl groups. This indicates a potential adsorbent material [36]. The preparation of rice husk as an inexpensive adsorbent will not only make efficient use of rice husk resources but will also promote the development of the rice husk industry and improve economic efficiency.

In this study, rice husk was used as the raw material, and KOH and KOH-NaOH were used as activators to prepare rice husk biochar for the adsorption of methylene blue. The effects of pyrolysis temperature, pyrolysis time and amount of activators on synthesis of biochar were investigated. The adsorption model and kinetic model of activated biochar for methylene blue were also studied. Furthermore, BET, FT-IR, and SEM were carried out to prove the feasibility of alternative preparation of traditional activated carbon materials from rice husk to achieve the purpose of agricultural waste utilization.

## 2. Experimental Section

*2.1. Materials and Instruments.* Rice husk comes from the College of Food Science and Engineering of Henan University of Technology. MB was purchased from Kemiou Chemical Reagent Co., Ltd, Tianjin. It was used as adsorbate. KOH, NaOH, HCl, and absolute ethyl alcohol were purchased from the local chemical dealer. These reagents used were of analytical grade.

GSL1200B tube furnace (Zhengzhou Kejing Electric Furnace Co., Ltd.) for rice husk pyrolysis; UV 6000 UV-Visible spectrophotometer (Shanghai Yuananalysis Instruments Co., Ltd.) for measuring MB; Micromeritics ASAP 2460 gas adsorption analyzer (Shanghai McMurritic Instruments Co., Ltd.) for determining specific surface area and porosity analysis; FEI Quanta FEG 250 scanning electron microscope (Zhejiang Nader Scientific Instruments Co., Ltd.) was used to observe the surface morphology of rice husk biochar; Perkin Elmer Spectrum FT-IR infrared spectrometer (Shanghai Perkin Elmer Enterprise Management Co., Ltd.) was used to analyze the structure of functional groups on the surface of rice husk biochar.

*2.2. Preparation of Rice Husk Biochar.* Rice husk was smashed to 30–40 mesh as raw material. KOH and KOH-NaOH were used as activators. Rice husk and activators were mixed according to different mass ratios in beakers. 50 mL of deionized water was added into the beakers to form suspension solution. The suspension solution was heated and stirred at 80°C on a magnetic stirrer for 1 h, then transferred to 100°C oven for 12 h. Finally, the modified rice husk was pyrolysed in a nickel ark and placed in a tube furnace. Nitrogen was selected as the protective gas and heated to different temperatures (700°C to 1000°C) at a heating rate of 10°C/min and kept for several hours (1 h to 3 h). After the tube furnace was naturally cooled to room temperature, the rice husk carbon was removed and washed several times with HCl (1 mol/L) solution to remove impurities, followed by several washes with hot distilled water and anhydrous

ethanol until the solution was neutral. Finally, the sample was placed in an oven at 100°C for 12 h to obtain activated biochar (KOH-activated biochar is denoted as K-AC, while KOH-NaOH-activated biochar is denoted as KN-AC.)

*2.3. Adsorption Experiments.* The adsorption experiments were performed by the batch method. Different amounts of K-AC or KN-AC were put into 150 mL flasks with 50 mL different initial concentrations of MB solution. The flasks were placed in thermostat shaker with 200 rpm at room temperature for different times. Separated by centrifuge at 8000 rpm for 3 min and the residual solution of MB was analyzed using UV 6000 at 664 nm. The adsorption capacity of MB ($q$) and the removal rate ($E$) were calculated according to (1) and (2), respectively

$$q_t = (C_0 - C) \times \frac{V}{m}, \quad (1)$$

$$E = \frac{(C_0 - C)}{C_0} \times 100\%, \quad (2)$$

where $q_t$ is the adsorption capacity of MB in mg/g; $C_o$ is the initial MB concentration in mg/L; $C$ is the final MB concentration in mg/L; $V$ is the volume of MB solution in $L$; m is the weight of adsorbent in $g$; $E$ is the removal rate of MB in %.

## 3. Results and Discussion

*3.1. Characterization of Samples.* Figure 1 shows the SEM image of activated biochar. Figure 1(a) shows that KN-AC is magnified 1000 times and has obvious porosity. Pyrolysis seriously damaged the surface fiber structure of rice husk. Figure 1(c) shows that KN-AC is magnified by 10000 times, and the surface holes are evenly distributed without obvious collapse. Figure 1(b) shows K-AC magnified by 1000 times, with rough surface and uneven distribution of surface holes. In particular, Figure 1(d) shows that K-AC is magnified by 10000 times, and the porosity is developed, but the collapse is obvious. It may be that the pyrolysis temperature is too high, resulting in the collapse of the original pores.

The nitrogen adsorption-desorption isotherms are shown in Figure 2. According to the IUPAC classification, the isotherms of KN-AC and K-AC both exhibit the characteristics of type I isotherms, with a sharp increase in nitrogen adsorption at relatively low pressure, indicating the presence of a large number of microspores, which is consistent with the SEM results.

As can be seen from Table 1, the specific surface area and microspore capacity of KN-AC are larger than those of K-AC. The structures of KN-AC and K-AC were investigated in detail using the $N_2$ adsorption-desorption isotherms at 77 K, as shown in Figure 2. The $N_2$ adsorption-desorption isotherms of KN-AC and K-AC are of type I. In the low relative pressure region, the adsorption capacity of KN-AC and K-AC increases sharply, which suggests that the adsorption characteristics of the samples are derived from the microspores. Figure 3 shows the pore size distribution of KN-AC and K-AC. Micropores were present in KN-AC and K-AC, mainly in the range of 2-3 nm, with more micropores in KN-AC than in K-AC, which is consistent with the results in Table 1.

*3.2. Effect of Mass Ratio of KN-AC and K-AC.* In KN-AC and K-AC activation experiments, 5 ratios were selected for research. The mass ratios taken in the KN-AC activation experiment are numbered as follows: no. 1 is 1 g rice husk: 0.1 g KOH + 0.9 g NaOH, no. 2 is 1 g rice husk: 0.3 g KOH + 0.7 g NaOH, no. 3 is 1 g rice husk: 0.5 g KOH + 0.5 g NaOH, no. 4 is 1 g rice husk: 0.7 g KOH + 0.3 g NaOH, and no. 5 is 1 g rice husk: 0.9 g KOH + 0.1 g NaOH. The mass ratio taken in the K-AC activation experiment was numbered as follows: no. 1 is 1 g rice husk: 2 g KOH, no. 2 is 1 g rice husk: 1 g KOH, no. 3 is 2 g rice husk: 1 g KOH, no. 4 is 3 g rice husk: 1 g KOH, and no. 5 is 4 g rice husk: 1 g KOH. Weigh 0.02 g KN-AC and K-AC, place them in 50 mL and 150 mg/L MB solution flasks, respectively, and adsorb them at 25°C for 4 hours. The results are shown in Figure 4. It can be seen that in the K-AC activation experiment, sample 1 and sample 2 have good adsorption capacity for MB, but the adsorption capacity of samples 3, 4, and 5 gradually decreases. This shows that too much activator will cause channel collapse and reduce specific surface area, thus reducing the adsorption performance of K-AC. In the KN-AC activation experiment, all samples showed excellent adsorption performance and slight difference. In contrast, sample 2 (i.e., the mass ratio of 1 g rice husk: 0.3 g KOH + 0.7 g NaOH) has the best adsorption capacity for methylene blue. The reason may be that the boiling point of potassium (762°C) is lower than that of sodium (882.9°C). When the activation temperature is lower than the boiling point of potassium, the two will be activated together to "establish pores" on the carbon body and form a preliminary pore structure (mainly micropores at this time). However, when the temperature is higher than the boiling point of potassium, the sodium vapor continues to "form pores," thus forming large micropores or mesopores. However, the doping ratio of NaOH in the activator should not be too high. If the content is too high, the activation effect will be reduced [37, 38].

*3.3. Effect of Pyrolysis Temperature of KN-AC and K-AC.* We investigated the effect of pyrolysis temperature of rice husk carbon (700°C, 800°C, 900°C, and 1000°C) on the adsorption performance of MB. In the KN-AC activation experiment, the selected mass ratio is 1 g rice husk: 0.3 g KOH + 0.7 g NaOH. In the activation experiment of K-AC, the selected mass ratio is 1 g rice husk: 1 g KOH. The adsorption conditions are the same as Section 3.2. The results are shown in Figure 5. It can be seen that in the KN-AC experiment, the best adsorption performance of KN-AC reached at the pyrolysis temperature of 800°C, which was 100°C lower than the best temperature of K-AC (900°C). However, with the increase in pyrolysis temperature, the adsorption performance of MB decreases significantly. This may be because the higher the temperature is, the greater the

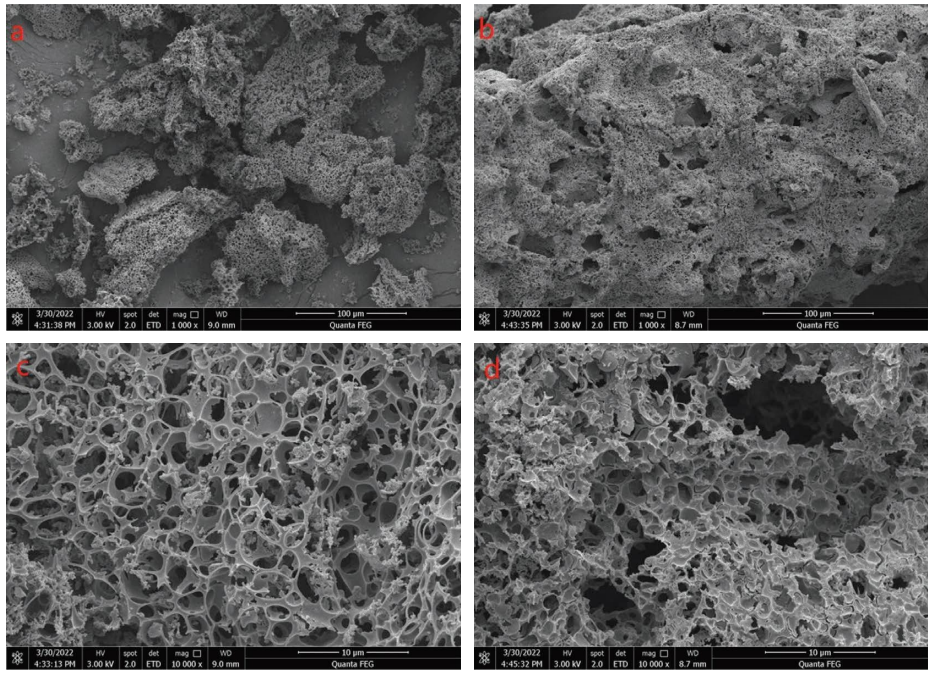


Figure 1: SEM images of K-AC and KN-AC ((a) ×1000 KN-AC, (b) ×1000 K-AC, (c) ×10000 KN-AC, and (d) ×10000 K-AC).

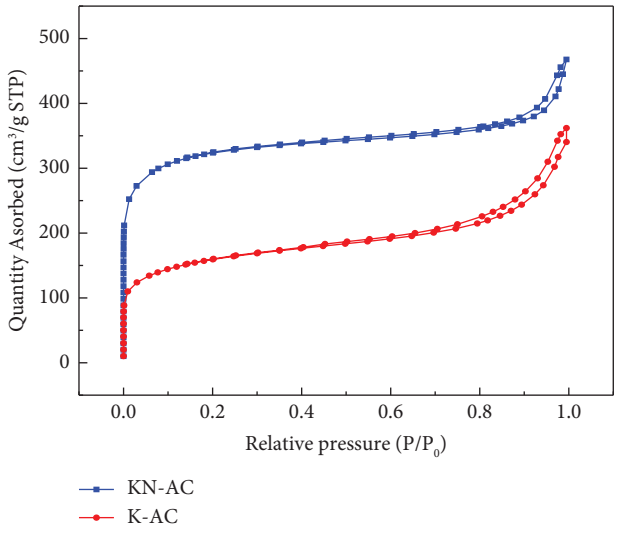


Figure 2: Nitrogen adsorption-desorption isotherms of the samples.

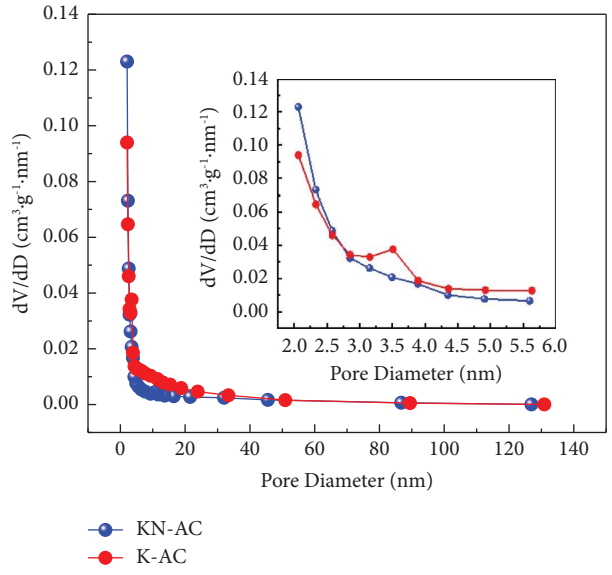


Figure 3: Pore size distribution curve of the sample.

Table 1: Textural parameters of samples.

| Samples | K-AC | KN-AC |
|---|---|---|
| BET ($m^2$/g) | 564 | 1196 |
| Total pore volume ($cm^3$/g) | 0.526 | 0.723 |
| Microporous pore volume ($cm^3$/g) | 0.173 | 0.447 |
| Average pore size (nm) | 3.734 | 2.418 |

excessive corrosion of sodium vapor on the carbon structure, leading to the collapse between the pore channels, a significant damage to the pore structure, and reduced adsorption capacity. In K-AC experiment, with the increase in pyrolysis temperature, the adsorption performance of MB first increased and then decreased, and showed the maximum adsorption performance when the pyrolysis temperature was 900°C. The possible reason is that the formation of the new microporous structure and the destruction of the previously generated microporous structure occur simultaneously during the pyrolysis process, and the previously generated microporous structure is significantly destroyed above 900°C.

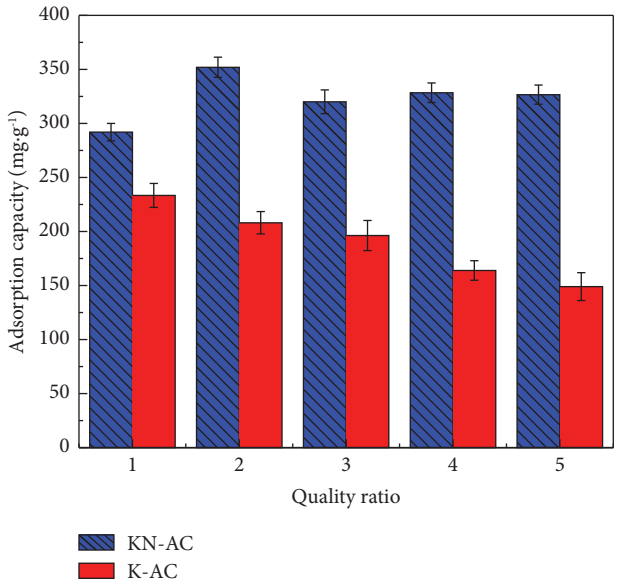


Figure 4: Effect of mass ratio of KN-AC and K-AC.

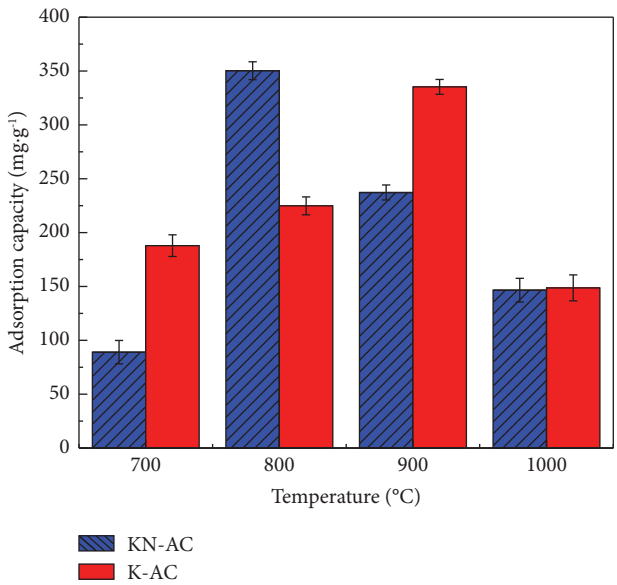


Figure 5: Effect of pyrolysis temperature of KN-AC and K-AC.

*3.4. Effect of Pyrolysis Time of KN-AC and K-AC.* We investigated the effect of pyrolysis time (1 h, 2 h and 3 h) of rice husk carbon on the adsorption performance of MB. In the KN-AC activation experiment, the selected mass ratio is 1 g rice husk: 0.3 g KOH + 0.7 g NaOH and the pyrolysis temperature is 800°C. In the activation experiment of K-AC, the selected mass ratio is 1 g rice husk: 1 g KOH and the pyrolysis temperature is 900°C. The adsorption conditions are the same as Section 3.2. The results are shown in Figure 6. It can be seen that the adsorption capacity of KN-AC decreases sharply with the increase in pyrolysis time. However, the adsorption capacity of K-AC decreased slowly with the increase in pyrolysis time. This may be because the longer

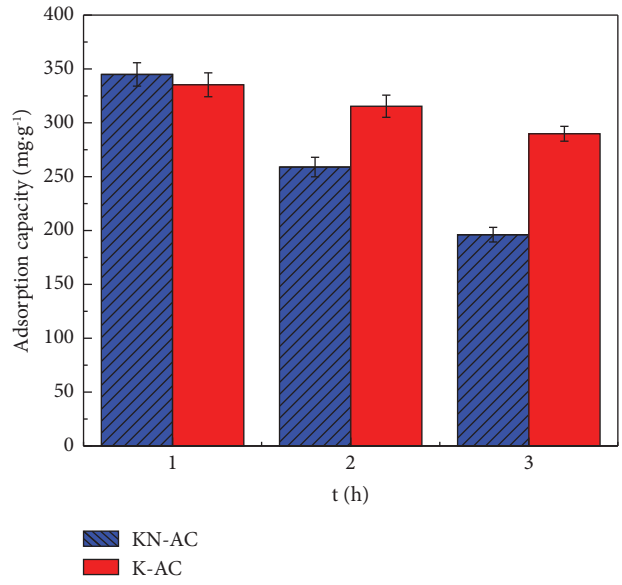


Figure 6: Effect of pyrolysis time of KN-AC and K-AC.

the pyrolysis time is, the more aggressive the sodium vapor is to the carbon structure than the potassium vapor. In addition, we found that the adsorption capacity of KN-AC prepared at 800°C for 1 h is higher than that of K-AC prepared at 900°C for 1 h, and the cost of NaOH is lower than that of KOH. This proves that activated biochar produced by the combined activation method has greater advantages and can reduce energy consumption [39].

*3.5. Effect of Solution pH.* Figure 7 shows the effect of adsorption of KN-AC and commercial samples on the MB at various pHs. The experiments were done at 25°C. 0.4 g/L KN-AC and commercial samples were placed in 150 mg/L methylene blue solution with pH values of 2, 4, 6, 8, and 10 for adsorption for three hours. In the pH range of 2–10, KN-AC adsorbed more than twice as much as the commercial sample. As the pH increased from 2 to 8, the adsorption capacity of KN-AC for MB continued to increase and the adsorption amount increased from 303.5 mg/g to 359.9 mg/g. The commercial samples showed the same pattern of adsorption as that of KN-AC. As the pH increased, the adsorption of the samples increased. There was maximum adsorption at a pH of 8. However, the commercial sample had a sorption of 173.3 mg/g at pH 8. According to a previous research [40], the increase in surface charge of the adsorbent as the pH of the solution increased resulted in a greater attraction between the functional groups on the adsorbent's surface and the MB molecules. This is because the presence of fewer $H^+$ ions reduces competition among the molecules of MB and $H^+$ ions, which increases the likelihood of electrostatic attraction. However, in our samples, we observed a decrease in adsorption at pH 9. This is consistent with the results of another study on MB adsorption with lignocellulosic adsorbents [41], which found that adsorption initially increased with the pH of the solution until it reached a maximum at pH 8 and then

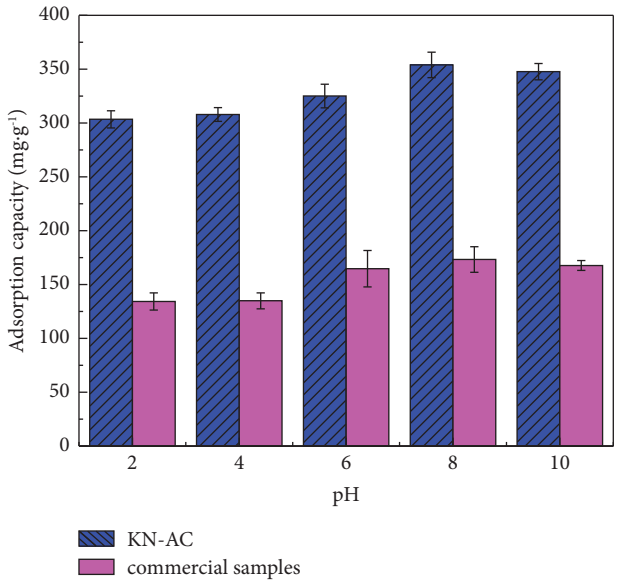


Figure 7: Effect of solution pH on the adsorption capacity of KN-AC and commercial samples.

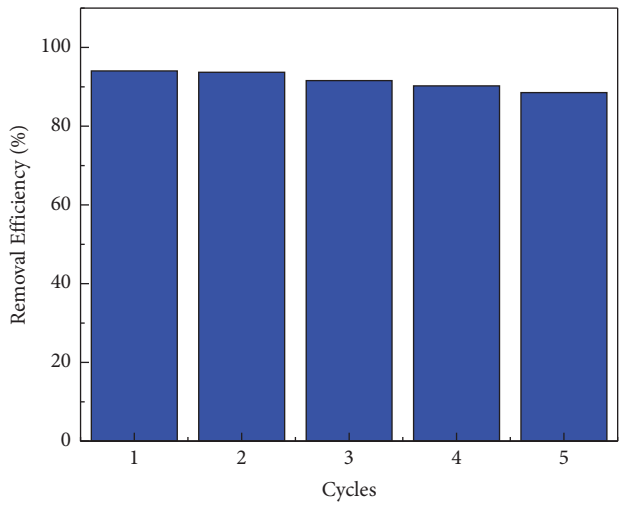


Figure 8: Regeneration cycle of KN-AC.

decreased at pH 9. This trend may be explained by the fact that at pH 9, there is less competition between the MB ions and the $H^+$ ions, which decreases the ionic strength of the solution and reduces the capacity of the adsorbent to bind MB ions on its surface.

*3.6. Desorption and Recovering.* In any adsorption process, the regeneration of the adsorbent is an important reference factor. In order to understand the regeneration capacity of KN-AC, we carried out an analytical study of it. First, 0.02 g of KN-AC was placed in 50 mL of 150 mg/L MB solution and reacted at room temperature for 12 h to saturate the adsorbent. KN-AC was then simply recovered by filtration through filter paper, rinsed several times with anhydrous ethanol and distilled water, dried at 110°C, and used again for MB dye wastewater. The adsorption conditions were the same as for the first adsorption. The results are shown in Figure 8. There was no significant loss of activity of KN-AC at the end of the fifth cycle. This proves that KN-AC can be reused.

*3.7. Comparison of KN-AC with Existing Adsorbents.* The adsorption efficiency of KN-AC for methylene blue dye obtained in this study was compared with other adsorbents reported in the literature (Table 2). The BET specific surface area and the maximum adsorption capacity were used as important parameters for comparison. It can be seen that the biomass activated carbon prepared with KOH as the activator had a larger specific surface area and was more effective in the adsorption of MB. The specific surface area values of KN-AC were very high compared to other adsorbents. There was also good adsorption of methylene blue. It can be used as a better adsorbent for the preparation of activated carbon.

*3.8. Adsorption Kinetics.* The adsorption kinetics of activated biochar was investigated at room temperature. A series of 0.02 g KN-AC with 0.3 KOH + 0.7 NaOH were added into a 150 mL flask with 50 mL of 150 mg/L of MB solution. Samples were taken at different times. In order to analyze the kinetics of MB adsorption on rice husk carbon, the pseudo-first-order model (PFO) and the pseudo-second-order model (PSO) were fitted, with the following expressions:

The pseudo-first-order model

$$\ln\left(q_e - q_t\right) = \ln q_e - K_1 t. \tag{3}$$

The pseudo-second-order model

$$\frac{t}{q_t} = \frac{1}{K_2 q_e^2} + \frac{t}{q_e}, \tag{4}$$

where $q_t$ is the adsorption amount in mg/g; $t$ is the adsorption time in min; $q_e$ is the equilibrium adsorption amount in mg/g; $K_1$ is the primary kinetic rate constant in $\min^{-1}$; $K_2$ is the secondary kinetic rate constant in $(g/(\text{mg}\bullet\ \text{min}))$.

Figure 9 shows the two kinetic models fitted to KN-AC. Figure 9(a) is the PFO, which has a correlation coefficient of $R^2 = 0.8398$ and $q_e(\text{cal}) = 341.261$ mg/g. Figure 9(b) is the PSO, which has a correlation coefficient of $R^2 = 0.999$ and $q_e(\text{cal}) = 360.780$ mg/g. It is clear that the experimental data from the PSO fit more smoothly than the results from the PFO. Furthermore, the experimental value $q_e(\text{exp}) = 359.7$ mg/g is the equilibrium adsorption amount when the KN-AC adsorbed MB reaches equilibrium, which is almost identical to the $q_e$(cal) for PSO. These results suggest that the PSO model is considered to be a better fitting model for describing the adsorption of MB on KN-AC and that the adsorption of MB is mainly controlled by chemisorption.

*3.9. Adsorption Isotherms.* To investigate the isothermal behavior of KN-AC with 0.3 KOH + 0.7 NaOH on MB adsorption, initial MB concentrations between 10 and 350 mg/L were put in flasks with stirring speed of 200 rpm

Table 2: Comparison of adsorption capacity of other work in the literature with KN-AC.

| Absorbent | Activating agents | Pyrolysis temperature (°C) | Surface area ($m^2 \cdot g^{-1}$) | $Q_{max}$ ($mg \cdot g^{-1}$) | Process parameters | | References |
|---|---|---|---|---|---|---|---|
| | | | | | Adsorbent dose ($g \cdot L^{-1}$) | pH | |
| Rice husk | KOH and NaOH | 800 | 1196 | 359.7 | 0.4 | 8 | This work |
| Corn cob | KOH | 700 | 492 | 333 | 0.8 | — | [42] |
| Soybean straw | KOH | 550 | 1906 | 1626.4 | 0.3 | 11 | [43] |
| Acacia wood | KOH | 550 | 1045 | 338.29 | 1 | 10 | [44] |
| Sweet potato vine | $ZnCl_2$ | 500 | 1397 | 299.2 | 1 | 12 | [45] |
| Prosopis juliflora stem | $ZnCl_2$ | 800 | 252 | — | 3.4 | — | [46] |
| Banana stem | $H_3PO_4$ | 400 | 837 | 101.01 | 1 | 7 | [47] |
| Waste pepper (isot) stems | $H_3PO_4$ | 650 | 1003 | 92.6 | 1 | 8 | [48] |
| Sugarcane | Natural zeolite | 500 | — | 51 | 0.1 | 7 | [49] |
| Industrial lignin | $FeCl_3 \cdot 6H_2O$ | 800 | 885 | 200 | 0.3–2.0 | 4 | [50] |
| Hickory chip | $H_2O_2$ | 450 | 143.3 | 310 | 0.4 | — | [51] |
| Watermelon rind | $H_2SO_4$ | 110 | 0.357 | 200 | 0.8 | 9 | [52] |
| Kelp | — | 1000 | 771 | 379.8 | 1 | — | [53] |

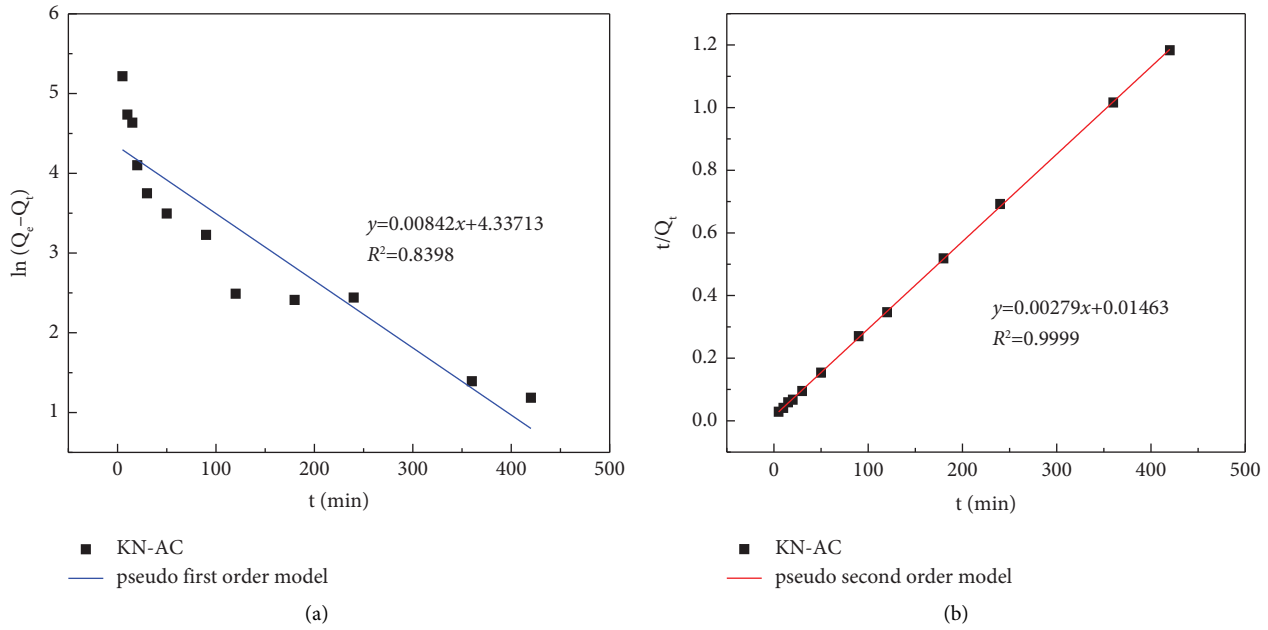


Figure 9: Pseudo-first-order (a) and pseudo-second-order (b) kinetic fitting curves of KN-AC.

for 3 h at 25°C. The adsorption isotherms of MB on KN-AC were fitted using the Langmuir and Freundlich model with the following expressions:

Langmuir isotherm equation

$$\frac{C_e}{q_e} = \frac{C_e}{q_m} + \frac{1}{k_L q_m}. \quad (5)$$

Freundlich isotherm equation

$$\ln q_e = \ln k_F + \frac{1}{n} \ln C_e, \quad (6)$$

where $C_e$ is the equilibrium concentration of MB in mg/L; $q_e$ is the adsorption capacity at equilibrium in mg/g; $q_m$ is the maximum adsorption capacity in mg/g; $k_L$ is the Langmuir adsorption equilibrium constant in L/mg; $k_F$ is the Freundlich adsorption equilibrium constant in L/mg; $n$ is the characteristic temperature-dependent constant; and $k_F$ and $n$ can be determined by the intercept and slope of the fitted straight line.

As can be seen from Figure 10(a), the adsorption process of KN-AC at different temperatures can be described by the Langmuir isotherm models. As can be seen from Figure 10(b), the adsorption process of KN-AC at different temperatures can be described by the Freundlich isotherm models. If the correlation coefficients ($R^2 = 0.999$) of the Langmuir model are closer to 1.0, then the adsorption of KN-AC is more in line with the Langmuir isotherm, and its adsorption process belongs to single molecular layer adsorption.

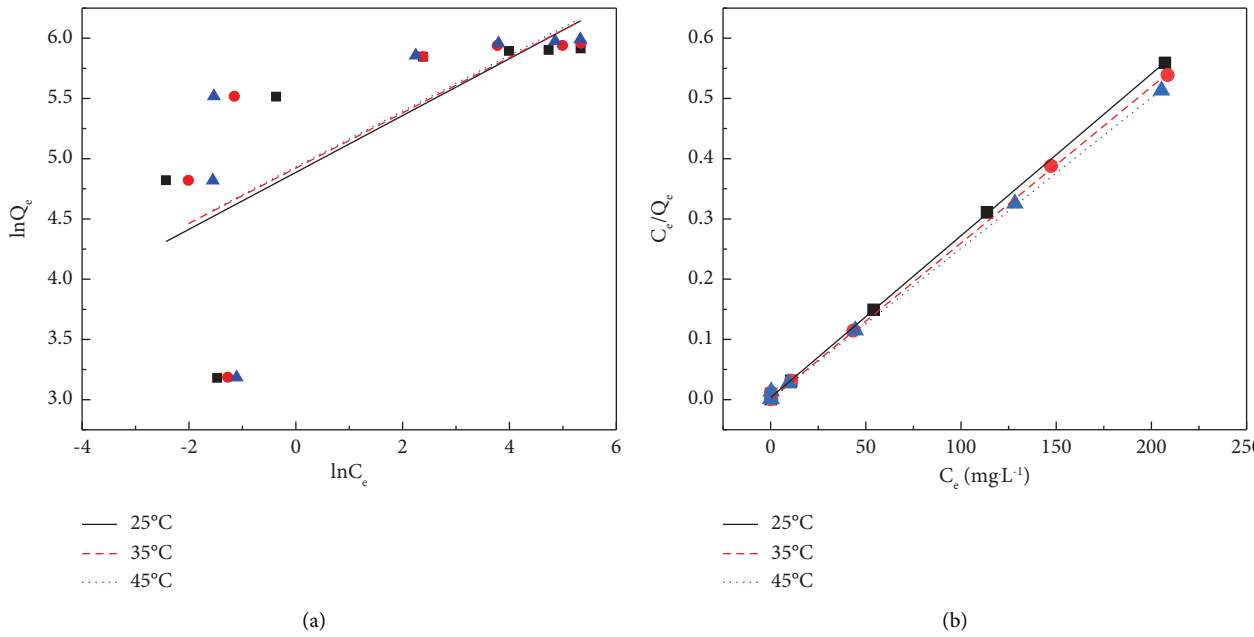


Figure 10: (a) Langmuir isotherm plots obtained for the adsorption MB onto KN-AC sorbent. (b) Freundlich isotherm plots obtained for the adsorption MB onto KN-AC.

Table 3: Thermodynamic parameters of adsorption of methylene blue by KN-AC.

| MB concentration (mg/L) | $H$ (kJ/mol) | $S$ (J/mol) | $G$ (kJ/mol) | | |
|---|---|---|---|---|---|
| | | | 298 K | 308 K | 318 K |
| 150 | 9.146 | 58.982 | −8.950 | −8.589 | −8.589 |
| 200 | 4.988 | 37.413 | −5.366 | −5.359 | −4.716 |
| 300 | 7.483 | 34.919 | −2.898 | −2.780 | −2.346 |

*3.10. Thermodynamic Studies.* In order to study the ability of KN-AC to adsorb methylene blue, the adsorption conditions at different temperatures were measured experimentally. The adsorption thermodynamic parameters ($\triangle G$, $\triangle H$, $\triangle S$) are used to characterize the influence of temperature on the adsorption effect. The calculation formula is as follows:

$$\begin{aligned} \Delta G &= \Delta H - T\Delta S, \\ \Delta G &= -RT\ln_{K_c}, \end{aligned} \tag{7}$$

where $K_c$ (value of $q_e/c_e$ of isotherm) is the sorption equilibrium constant; $R$ is the ideal gas constant [8.314 $j/(\text{mol}\bullet K)$]; $T$ is the absolute temperature in $K$.

Other thermodynamic parameters, including enthalpy change $\Delta H$ and entropy change $\Delta S$ of MB adsorption value, calculate the slope and intercept of $\ln K_c$ and $1/T$ curve with van Hoff equation, as follows:

$$\ln K_c = -\frac{\Delta H}{R} \bullet \frac{1}{T} + \frac{\Delta S}{R}. \tag{8}$$

Table 3 shows that the enthalpy of $\Delta H$ is positive, indicating that the adsorption is a heat absorption process. Furthermore, the adsorption values of KN-AC for methylene blue increased with increasing temperature. This proves the importance of temperature in the adsorption process. The $\Delta S$ value for entropy is also positive, indicating that higher temperatures promote disorder at the solid-liquid interface. On the other hand, $\Delta G$ is negative, implying that the adsorption process of MB on KN-AC is spontaneous. Furthermore, $\Delta G$ increases with increasing temperature, suggesting that higher temperatures increase the reaction driving force and thus promote adsorption. From these results, it is clear that temperature plays a key role in the adsorption process of KN-AC.

## 4. Conclusion

KOH and KOH-NaOH rice husk AC were produced via the two-step method. The MB adsorption studies demonstrated that the specific surface area and adsorption capacity of KN-AC (specific surface area 1196 $m^2/g$, $q = 359.7$ mg/g) were increased compared with those of K-AC (specific surface area 564 $m^2/g$, $q = 315.4$ mg/g). The combined activation not only solves the problem of KOH being environmentally unfriendly and lacking NaOH etching ability but also reduces the cost and energy consumption while maintaining a good adsorption effect. In addition, these findings indicate that rice husk is an excellent raw material

for preparing nanoporous activated biochar and has great potential in the wider application of biomass.

## Data Availability

The data used to support the findings of this study are available from the corresponding author upon request.

## Conflicts of Interest

The authors declare that they have no conflicts of interests.

## Authors' Contributions

Author 1 (Dan Dang): Conceptualization, Methodology, Investigation, Formal Analysis, Funding Acquisition, Writing-Review & Editing. Author 2 (Lei Mei): Investigation, Data Curation, Formal Analysis, Writing-Original Draft; Author 3 (Gaimeng Yan): Writing-Review, Data Curation & Editing; Author 4 (Wenju Liu): Conceptualization, Resources, Supervision, Review & Editing.

## Acknowledgments

This study was supported by the Science and Technology Foundation of Henan Province (No. 232102320217).

## References

[1] H. A. Chauhan, M. Rafatullah, K. A. Ali, M. F. Umar, M. A. Khan, and B. H. Jeon, "Photocatalytic Activity Of Graphene Oxide/Zinc Oxide Nanocomposite Derived From Rice Husk For The Degradation Of Phenanthrene Under Ultraviolet-Visible Light," *Journal of Water Process Engineering*, vol. 47, Article ID 102714, 2022.

[2] A. Yeganeh, G. Nabi-Bidhendi, H. Rashedi, and M. Hosseinzadeh, "Development Of Membrane Bioreactor To Membrane Electro-Bioreactor For Advanced Treatment Of Wastewater," *Pollution*, vol. 6, pp. 197–210, 2020.

[3] R. Natarajan and R. Manivasagan, "Effect Of Operating Parameters On Dye Wastewater Treatment Using Prosopis Cineraria And Kinetic Modeling," *Environmental Engineering Research*, vol. 25, no. 5, pp. 788–793, 2019.

[4] R. T. Kapoor, M. Rafatullah, M. R. Siddiqui, M. A. Khan, and M. Sillanpää, "Removal of reactive black 5 dye by banana peel biochar and evaluation of its phytotoxicity on tomato," *Sustainability*, vol. 14, no. 7, p. 4176, 2022.

[5] S. Sahu, S. Pahi, S. Tripathy et al., "Adsorption of methylene blue on chemically modified lychee seed biochar: dynamic, equilibrium, and thermodynamic study," *Journal of Molecular Liquids*, vol. 315, Article ID 113743, 2020.

[6] F. Uddin, "Environmental hazard in textile dyeing wastewater from local textile industry," *Cellulose*, vol. 28, no. 17, Article ID 10715, 10739 pages, 2021

[7] N. A. Akbar, N. D. Rosman, S. Hambali, and A. A. Abu Bakar, "Adsorption of methylene blue by banana stem adsorbent in a continuous fixed bed column study," *IOP Conference Series: Earth and Environmental Science*, vol. 616, no. 1, Article ID 12058, 2020.

[8] F. Ding, T. Shen, Q. Zhao, X. Jin, S. Mao, and M. Gao, "Series of bis-morpholinium-basedorgano-Vts for the removal of anionic dyes," *Journal of Molecular Liquids*, vol. 360, Article ID 119424, 2022.

[9] B. P. Thillainayagam, R. Nagalingam, and P. Saravanan, "Batch and Column Studies on Removal of Methylene Blue Dye by Microalgae Biochar," *Biomass Conversion and Biorefinery*, pp. 1–16, 2022.

[10] T. V. Tan and H. T. T. Nguyen, "Activated carbon based rice husk for highly efficient adsorption of methylene blue: kinetic and isotherm," *IOP Conference Series: Materials Science and Engineering*, vol. 1092, no. 1, Article ID 12078, 2021.

[11] J. M. Jabar, Y. A. Odusote, Y. T. Ayinde, and M. Yılmaz, "African almond (*Terminalia catappa* L) leaves biochar prepared through pyrolysis using H3PO4 as chemical activator for sequestration of methylene blue dye," *Results in Engineering*, vol. 14, Article ID 100385, 2022.

[12] Q. Han, J. Wang, B. A. Goodman, J. Xie, and Z. Liu, "High adsorption of methylene blue by activated carbon prepared from phosphoric acid treated eucalyptus residue," *Powder Technology*, vol. 366, pp. 239–248, 2020.

[13] H. N. Hamad and S. Idrus, "Recent developments in the application of bio-waste-derived adsorbents for the removal of methylene blue from wastewater: a Review," *Polymers*, vol. 14, no. 4, p. 783, 2022.

[14] S. Gao, L. Liu, Y. Tang, D. Jia, Z. Zhao, and Y. Wang, "Coal based magnetic activated carbon as a high performance adsorbent for methylene blue," *Journal of Porous Materials*, vol. 23, no. 4, pp. 877–884, 2016.

[15] H. Roy, T. R. Prantika, M. H. Riyad, S. Paul, and M. S. Islam, "Synthesis, characterizations, and RSM analysis of Citrus macroptera peel derived biochar for textile dye treatment," *South African Journal of Chemical Engineering*, vol. 41, pp. 129–139, 2022.

[16] X. Bai, B. Quan, C. Kang et al., "Activated Carbon from tea Residue as Efficient Absorbents for Environmental Pollutant Removal from Wastewater," *Biomass Conversion and Biorefinery*, pp. 1–10, 2022.

[17] N. Bagheri and J. Abedi, "Preparation of high surface area activated carbon from corn by chemical activation using potassium hydroxide," *Chemical Engineering Research and Design*, vol. 87, no. 8, pp. 1059–1064, 2009.

[18] S. A. Alshareef, M. Otero, H. S. Alanazi, M. R. Siddiqui, M. A. Khan, and Z. A. Alothman, "Upcycling olive oil cake through wet torrefaction to produce hydrochar for water decontamination," *Chemical Engineering Research and Design*, vol. 170, pp. 13–22, 2021.

[19] O. O. Namal and E. Kalipci, "Adsorption kinetics of methylene blue removal from aqueous solutions using potassium hydroxide (KOH) modified apricot kernel shells," *International Journal of Environmental Analytical Chemistry*, vol. 100, no. 14, pp. 1549–1565, 2019.

[20] İ. Teğin, M. F. Demirel, İ. Alacabey, and E. Yabalak, "Investigation of the Effectiveness of Waste Nut Shell–Based Hydrochars in Water Treatment: A Model Study for the Adsorption of Methylene Blue," *Biomass Conversion and Biorefinery*, pp. 1–14, 2022.

[21] Y. Wang, C. Srinivasakannan, H. Wang et al., "Preparation of novel biochar containing graphene from waste bamboo with high methylene blue adsorption capacity," *Diamond and Related Materials*, vol. 125, Article ID 109034, 2022.

[22] U. D. Hamza, N. S. Nasri, N. S. Amin, J. Mohammed, and H. M. Zain, "Characteristics of oil palm shell biochar and activated carbon prepared at different carbonization times," *Desalination and Water Treatment*, vol. 57, no. 17, pp. 7999–8006, 2015.

[23] Y. Tang, Y. Zhao, T. Lin, Y. Li, R. Zhou, and Y. Peng, "Adsorption performance and mechanism of methylene blue

by H3PO4- modified corn stalks," *Journal of Environmental Chemical Engineering*, vol. 7, no. 6, Article ID 103398, 2019.

[24] A. J. Kumar and C. Namasivayam, "Uptake of endocrine disruptor bisphenol-A onto sulphuric acid activated carbon developed from biomass: equilibrium and kinetic studies," *Sustainable Environment Research*, vol. 24, no. 1, pp. 73–80, 2014.

[25] A. J. Kumar, R. P. Singh, D. Fu, and C. Namasivayam, "Comparison of physical-and chemical-activated Jatropha curcas husk carbon as an adsorbent for the adsorption of Reactive Red 2 from aqueous solution," *Desalination and Water Treatment*, vol. 95, pp. 308–318, 2017.

[26] S. Wang, Y. R. Lee, Y. Won et al., "Development of high-performance adsorbent using KOH-impregnated rice husk-based activated carbon for indoor CO2 adsorption," *Chemical Engineering Journal*, vol. 437, Article ID 135378, 2022.

[27] J. S. Cha, S. H. Jang, S. S. Lam et al., "Performance of CO2 and Fe-modified lignin char on arsenic (V) removal from water," *Chemosphere*, vol. 279, Article ID 130521, 2021.

[28] A. H. Jawad, A. Saud Abdulhameed, L. D. Wilson, S. S. A. Syed-Hassan, Z. A. Alothman, and M. Rizwan Khan, "High surface area and mesoporous activated carbon from KOH-activated dragon fruit peels for methylene blue dye adsorption: optimization and mechanism study," *Chinese Journal of Chemical Engineering*, vol. 32, pp. 281–290, 2021.

[29] A. Malik, A. Khan, N. Anwar, and M. Naeem, "A comparative study of the adsorption of Congo red dye on rice husk, rice husk char and chemically modified rice husk char from aqueous media," *Bulletin of the Chemical Society of Ethiopia*, vol. 34, no. 1, pp. 41–54, 2020.

[30] T. H. Do, V. T. Nguyen, N. Q. Dung et al., "Study on methylene blue adsorption of activated carbon made from Moringa oleifera leaf," *Materials Today: Proceedings*, vol. 38, pp. 3405–3413, 2021.

[31] T. Alfatah, E. M. Mistar, and M. D. Supardan, "Porous structure and adsorptive properties of activated carbon derived from Bambusa vulgaris striata by two-stage KOH/NaOH mixture activation for Hg2+ removal," *Journal of Water Process Engineering*, vol. 43, Article ID 102294, 2021.

[32] H. Zhao, H. Zhong, Y. Jiang et al., "Porous ZnCl2-activated carbon from shaddock peel: methylene blue adsorption behavior," *Materials*, vol. 15, no. 3, p. 895, 2022.

[33] W. Zhang, Y. Wang, L. Fan et al., "Sorbent properties of orange peel-based biochar for different pollutants in water," *Processes*, vol. 10, no. 5, p. 856, 2022.

[34] A. Aldawsari, M. Ali Khan, B. H. Hameed et al., "Development of activated carbon from Phoenix dactylifera fruit pits: process optimization, characterization, and methylene blue adsorption," *Desalination and Water Treatment*, vol. 62, pp. 273–281, 2017.

[35] J. Sastré-Hernández, J. R. Aguilar-Hernández, J. Santoyo-Salazar et al., "Influence of sodium peroxide during the synthesis of SiO2 obtained from rice husk," *Materials Science in Semiconductor Processing*, vol. 114, Article ID 105087, 2020.

[36] P. S. Keng, S. L. Lee, S. T. Ha, Y. T. Hung, and S. T. Ong, "Removal of hazardous heavy metals from aqueous environment by low-cost adsorption materials," *Environmental Chemistry Letters*, vol. 12, no. 1, pp. 15–25, 2014.

[37] Y. H. Zhang, J. P. Wang, and Z. H. Jin, "Preparation of C/C composites by thermal gradient chemical vapor infiltration with vaporized kerosene as a precursor," *Carbon*, vol. 48, no. 10, pp. 3004-3005, 2010.

[38] R. K. Liew, E. Azwar, P. N. Y. Yek et al., "Microwave pyrolysis with KOH/NaOH mixture activation: a new approach to produce micro-mesoporous activated carbon for textile dye adsorption," *Bioresource Technology*, vol. 266, pp. 1–10, 2018.

[39] W. Jiang, X. Xing, X. Zhang, X. Zhang, and M. Mi, "Analysis of preparation and combustion characteristics of NaOH/KOH catalyzed straw pyrolytic carbon," *Journal of Thermal Analysis and Calorimetry*, vol. 136, no. 2, pp. 803–813, 2018.

[40] M. S. Sajab, C. H. Chia, S. Zakaria, and P. S. Khiew, "Cationic and anionic modifications of oil palm empty fruit bunch fibers for the removal of dyes from aqueous solutions," *Bioresource Technology*, vol. 128, pp. 571–577, 2013.

[41] M. S. Sajab, C. H. Chia, S. Zakaria et al., "Citric acid modified kenaf core fibres for removal of methylene blue from aqueous solution," *Bioresource Technology*, vol. 102, no. 15, pp. 7237–7243, 2011.

[42] A. Medhat, H. H. El-Maghrabi, A. Abdelghany et al., "Efficiently activated carbons from corn cob for methylene blue adsorption," *Applied Surface Science Advances*, vol. 3, Article ID 100037, 2021.

[43] Y. Ge, Y. Wang, G. Xu, and Z. Fang, "Preparation of activated carbon from soybean straw for high-efficiency adsorption methylene blue in aqueous solution," *Water, Air, & Soil Pollution*, vol. 234, no. 2, p. 74, 2023.

[44] M. F. M. Yusop, M. A. Ahmad, N. A. Rosli, and M. E. A. Manaf, "Adsorption of cationic methylene blue dye using microwave-assisted activated carbon derived from acacia wood: optimization and batch studies," *Arabian Journal of Chemistry*, vol. 14, no. 6, Article ID 103122, 2021.

[45] W. Zhang, Y. Zhao, Q. Liao, Z. Li, D. Jue, and J. Tang, "Sweet-potato-vine-Basedhigh-performance porous carbon for methylene blue adsorption," *Molecules*, vol. 28, no. 2, p. 819, 2023.

[46] N. Vasiraja, R. S. S. Prabhahar, and A. Joshua, "Preparation and Physio–Chemical characterisation of activated carbon derived from prosopis juliflora stem for the removal of methylene blue dye and heavy metal containing textile industry effluent," *Journal of Cleaner Production*, vol. 397, Article ID 136579, 2023.

[47] E. Misran, O. Bani, E. M. Situmeang, and A. S. Purba, "Banana stem based activated carbon as a low-cost adsorbent for methylene blue removal: isotherm, kinetics, and reusability," *Alexandria Engineering Journal*, vol. 61, no. 3, pp. 1946–1955, 2022.

[48] H. Dolas, "Activated Carbon Synthesis and Methylene Blue Adsorption from Pepper Stem Using Microwave Assisted Impregnation Method: Isotherm and Kinetics," *Journal of King Saud University-Science*, vol. 35, Article ID 102559, 2023.

[49] F. Mohamed, M. Shaban, S. K. Zaki et al., "Activated carbon derived from sugarcane and modified with natural zeolite for efficient adsorption of methylene blue dye: experimentally and theoretically approaches," *Scientific Reports*, vol. 12, no. 1, Article ID 18031, 2022.

[50] Y. Sun, T. Wang, C. Han et al., "Facile synthesis of Fe-modified lignin-based biochar for ultra-fast adsorption of

methylene blue: selective adsorption and mechanism studies," *Bioresource Technology*, vol. 344, Article ID 126186, 2022.

[51] Y. Zhang, Y. Zheng, Y. Yang et al., "Mechanisms and adsorption capacities of hydrogen peroxide modified ball milled biochar for the removal of methylene blue from aqueous solutions," *Bioresource Technology*, vol. 337, Article ID 125432, 2021.

[52] A. H. Jawad, R. Razuan, J. N. Appaturi, and L. D. Wilson, "Adsorption and mechanism study for methylene blue dye removal with carbonized watermelon (*Citrullus lanatus*) rind prepared via one-step liquid phase H2SO4 activation," *Surfaces and Interfaces*, vol. 16, pp. 76–84, 2019.

[53] M. Luo, L. Wang, H. Li, Y. Bu, Y. Zhao, and J. Cai, "Hierarchical porous biochar from kelp: insight into self-template effect and highly efficient removal of methylene blue from water," *Bioresource Technology*, vol. 372, Article ID 128676, 2023.